Acta Chemica Scandinavica, 1995: 49: 417–422
Printed in Belgium – all rights reserved

ACTA
CHEMICA SCANDINAVICA
ISSN 0904–213X

Synthesis and Crystal Structure of $V_{15}Sb_{18}$

Sigrid Furuseth† and Helmer Fjellvåg

Department of Chemistry, University of Oslo, N-0315 Oslo, Norway

Furuseth, S. and Fjellvåg, H., 1995. Synthesis and Crystal Structure of $V_{15}Sb_{18}$. – Acta Chem. Scand. 49: 417–422 © Acta Chemica Scandinavica 1995.

The 'new' phase $V_{15}Sb_{18}$ has been synthesized as polycrystalline powder and as single crystals by means of chemical transport reactions. $V_{15}Sb_{18}$ is shown to be the correct formula for the phase described as V_5Sb_4 in the literature, and most probably there exists no phase with a Ti_5Te_4-type crystal structure as assumed earlier. $V_{15}Sb_{18}$ crystallizes in space group $P4/nmm$ with $a = 958.66 \pm 0.05$ and $c = 704.74 \pm 0.05$ pm. Its crystal structure was solved on the basis of single-crystal X-ray diffraction data ($R = 0.030$). One of the vanadium sites (in position $2c$) is half-filled. This special feature was verified for another single crystal which was grown without iodine as transporting agent. According to data for powder samples with different nominal compositions, the phase has no major range of homogeneity. The phase exhibits weak, almost temperature-independent paramagnetism. At high temperatures, $T = 1205 \pm 10$ K, $V_{15}Sb_{18}$ decomposes peritectoidally into VSb_2 and $V_{1.4}Sb$ (NiAs-type). The atomic arrangement shows structural elements typical both for VSb_2 and for V_3Sb ($CuAl_2$-type and Cr_3Si-type, respectively). Two types of columns of coordination polyhedra running along [001] are identified, columns of V tetrahedra connected by Sb atoms, and columns of distorted, square antiprismatic V–Sb units ($[V_2Sb_8]_n$ chains). The relationship between the antiprismatic building units of $V_{15}Sb_{18}$, VSb_2 and VS_4 is described. The metal–metal bonding is extensive. The V_4 tetrahedra are connected by 'single' V atoms forming a two-dimensional network of V–V close contacts (268–295 pm).

The phase relations in the V–Sb system, in particular for the region around 50 atom% Sb, are more complex than for other 3d-metal antimonides. Typically, phases around the 1:1 composition in transition-metal pnictides either take the MnP-type structure (mainly phosphides and arsenides) or the NiAs-type structure, the latter phases frequently exhibiting a substantial range of non-stoichiometry. There is consensus in the literature that an NiAs-type phase also occurs in the V–Sb system, however, with a composition around $V_{1.4}Sb$.[1]

In the V–Sb system the phases V_3Sb,[2] V_3Sb_2[3] (in earlier studies termed V_6Sb_5),[4] $V_{1.4}Sb$,[1,4,5] V_5Sb_4[6] and VSb_2[7] have been reported. For all of these, except V_5Sb_4, convincing structure determinations are available. Eberle and Schubert[6] reported in 1968 the existence of a phase with a composition close to VSb that crystallizes with the Ti_5Te_4-type structure. This phase has later been described as V_5Sb_4 in the literature. Bouwma *et al.*[1] were not able to observe V_5Sb_4 in samples quenched from 1373 K. However, the present reinvestigation of the V–Sb system revealed that for annealing conditions below 1205 K, a phase with unit-cell dimensions closely resembling those earlier reported for V_5Sb_4 is obtained. However, the analysis of the single-crystal X-ray diffraction data showed that the true composition is $V_{15}Sb_{18}$, and that the crystal structure actually has no major resemblance to the Ti_5Te_4-type structure. The present paper reports on the preparation, crystal structure, stability and magnetic properties of $V_{15}Sb_{18}$.

Experimental

Sample preparation. Samples with composition $V_{0.70}Sb$–$V_{1.30}Sb$ were prepared by heating weighed amounts of the elements (V, 99.5%, A.D. Mackay; Sb, 99.995% Riedel-de Haën) in evacuated and sealed silica glass ampoules. The samples were first heated at 1200 K for 4 days and at 1125 K for 7 days, then crushed and heated to 1125 K for 7 days before finally being quenched in ice water. Additional samples were prepared, for which either a higher quenching temperature was used (up to 1375 K), or slow cooling (down to room temperature over 3 weeks) was adopted.

Single crystals were grown by chemical vapour transport reaction with iodine as a transport agent. 5 mg I_2 per cm^3 ampoule volume was used, the transport distance was 12 cm, and the temperature was 1125 K in the growth zone and 1175 K in the hot part of the ampoule. A multiphase powder sample with nominal composition VSb was used as reactant. Polyhedral single crystals with dimensions up to 3 mm in cross-section and with metallic

† To whom correspondence should be addressed.

lustre were obtained. In experiments where no transport agent was used, tiny single crystals (with maximum cross-section 0.1 mm) were obtained in the powder samples after prolonged heat treatment (4 months at 1125 K).

Characterization. All powder samples were characterized by powder X-ray diffraction (PXD), using a Guinier–Hägg camera with Cu $K\alpha_1$ radiation and Si as internal standard. Unit-cell dimensions were obtained by least-squares refinements of PXD data, using the CELLKANT program.[8]

The single crystals were investigated by optical microscopy, and the single crystals, as well as the starting materials, were further analyzed by scanning electron microscopy (SEM) and energy-dispersive X-ray analysis (EDX).

Magnetic susceptibility data were collected at a magnetic field of 500 Oe, between 5 and 325 K with a SQUID magnetometer (MPMS, Quantum Design).

X-Ray intensity data collection. Single-crystal X-ray intensity data were collected with Mo$K\alpha$ radiation at 295 K with a Nicolet P3/F diffractometer in the θ–2θ scan mode. Data were collected for scattering angles up to $2\theta = 70°$ at a scan speed of 2.00° min^{-1}. For a single crystal with dimensions $0.1 \times 0.1 \times 0.05$ mm^3, grown by chemical transport reaction, 5506 reflections with $I > 3\sigma(I)$ were recorded, giving 835 unique reflections. For a smaller crystal, with dimensions $0.05 \times 0.03 \times 0.01$ mm^3, grown without transport agent, 5432 reflections were similarly measured to give a data set of 782 unique reflections. The intensity data were corrected for Lorentz and polarization effects, absorption, and isotropic extinction. Least-squares refinements were performed, minimizing $\Sigma w(|F_o| - |F_c|)^2$ with weight $w = 1/\sigma^2(F_o)$. For all calculations, the GX program system[9] was used. Relevant data for the structure analysis are shown in Table 1.

Table 1. Crystal data.

Compound	$V_{15}Sb_{18}$
Crystal system	Tetragonal
a/pm	958.66(5)
c/pm	704.74(5)
Cell volume/pm^3	647.7(1)
Space group	*P*4/*nmm* (No. 129)
Z	1
d_{calc}/g cm^{-3}	7.576(2)
Crystal shape	Polyhedral
Crystal dimensions/mm	0.1×0.1×0.05
Linear absorption coefficient μ/cm^{-1}	239
Diffractometer	Nicolet P3/F
Radiation	Mo$K\alpha$
Scan mode	θ–2θ
Experimental temperature/K	295
Scan speed/° min^{-1}	2.00
Scan range/°	0.8–0.8
Background count time/scan time	0.50
2θ-range/°	0–70.0
Range of *h*, *k* and *l*	−15 to 15; −15 to 15 and −12 to 12
No. of collected reflections	6012
No. of observed; $I > 3\sigma(I)$	5506
No. of unique reflections	835
Test reflections	3
Absorption correction	Empirical (DIFABS)
Min. and max. absorption correction	0.827 and 1.396
Structure determination	MITHRIL/Fourier
Structure refinement minimizing	$\Sigma w(\|F_o\| - \|F_c\|)^2$
Weighting scheme	$w = 1/\sigma^2(F_o)$
R	0.030
R_w	0.031

Results and discussion

Phase relations. The PXD data for samples prepared at 1200 K with compositions around VSb were not in accordance with published diffraction patterns for any well described V–Sb phase. For a sample with nominal composition $V_{0.9}Sb$, no Bragg reflections from any of the phases V_3Sb, V_3Sb_2, $V_{1.4}Sb$ and VSb_2 were observed, and based on microscopy studies the sample was considered to be close to single phase. The diffraction pattern resembled that reported by Eberle and Schubert for V_5Sb_4.[6] However, the present phase analysis clearly showed that the actual phase has a higher antimony content than $4/9 \times 100$ atom%. Indexing the unknown powder diffraction pattern was simple, and was verified by trial-and-error indexing using the TREOR program,[10] to give a tetragonal unit cell with $a = 958.34 \pm 0.05$ and $c = 705.36 \pm 0.05$ pm, with figure of merit, $M(20) = 302$.[11]

Relative integrated intensities (obtained by microdensitometer readings of the Guinier films and the SCANPI program system),[12] *d*-values and Miller indices are given in Table 2. Later, it proved possible to obtain single crystals of this new phase by chemical transport reactions, using iodine as the transporting agent, and data from

Table 2. Observed Bragg reflections for $V_{15}Sb_{18}$ as measured by microdensitometer. *d*-values, relative intensities, and Miller indices (*hkl*).

d/pm	Rel. int.	*hkl*	*d*/pm	Rel. int.	*hkl*
352.3	0.07	002	205.9	0.06	213
330.5	0.39	102	205.1	0.30	421
305.5	0.35	221	193.0	0.29	223
303.2	0.27	310	176.0	0.03	004
291.1	0.48	301	173.2	0.12	104
278.5	0.29	311	169.5	0.15	440
272.1	0.31	212	168.4	0.17	432/502
248.8	1.00	321	167.7	0.27	403
244.3	0.53	222	162.8	0.14	333
239.7	0.21	400	160.1	0.09	531
236.7	0.50	302	159.8	0.10	600
227.0	0.13	401	188.9	0.06	522
226.0	0.15	330	155.7	0.09	601
221.9	0.15	113	153.8	0.08	611
220.8	0.60	411	151.6	0.05	620
210.9	0.26	203			

Table 3. Refined atomic parameters for $V_{15}Sb_{18}$, space group *P4/nmm*. Calculated standard deviations in parentheses. Data for one single crystal, grown by chemical transport reaction, are given, see text.

Atom	Wyckoff position	*x*	*y*	*z*	U_{iso} [a]
Sb(1)	2*c*	3/4	1/4	1/2	52(3)
Sb(2)	8*j*	−0.0835(1)	−0.0835(1)	0.3562(1)	30(2)
Sb(3)	8*i*	3/4	−0.0116(1)	0.8165(1)	21(2)
0.46(3) V(1)	2*c*	1/4	1/4	0.9239(6)	107(16)
V(2)	2*c*	1/4	1/4	0.4103(4)	9(4)
V(3)	4*d*	1/2	0	0	18(4)
V(4)	8*i*	3/4	0.3900(1)	0.1603(3)	22(3)

[a] $U_{iso}=\frac{1}{3}\Sigma\Sigma\ U_{ij}\ a_i^*\ a_j^*\ \boldsymbol{a}_i\boldsymbol{a}_j$.

Weissenberg photographs confirmed the unit-cell dimensions.

The obtained unit-cell dimensions resemble (as a multiple cell, double *c*-axis) those expected for a Ti_5Te_4-type[13] phase. Single-crystal data (Weissenberg) for a phase with assumed composition V_5Sb_4 were refined by Eberle and Schubert[6] in space group *I*4/*m*, $a = 981$ and $c = 350$ pm, to yield $R = 0.33$ for a Ti_5Te_4-type atomic arrangement. The similarities in the powder diffraction pattern, and the poor fit of the observed diffraction intensities to a Ti_5Te_4-type structure model in the earlier work,[6] indicate that the phase presently described as $V_{15}Sb_{18}$ may actually be the phase V_5Sb_4 reported in the literature. During this work it was not possible to obtain any phase with unit-cell dimensions corresponding to literature data for V_5Sb_4.

Based on data from thermal analysis (DTA) and examination of samples quenched from different temperatures, $V_{15}Sb_{18}$ was found to exist up to 1205 ± 10 K. PXD data of samples investigated by DTA and taken out just after the endothermal effect observed at 1205 K, showed that $V_{15}Sb_{18}$ decomposes peritectoidally into $V_{1.4}Sb$ (NiAs-type) and VSb_2. In addition, some Bragg reflections from the low-temperature phase V_3Sb_2 were observed together with some faint diffraction lines due to $V_{15}Sb_{18}$. This shows that during cooling $V_{1.4}Sb$ decomposes eutectoidally into V_3Sb_2 and $V_{15}Sb_{18}$; however, the degree of transformation is limited by the rather rapid cooling adopted. These observations fit earlier literature reports and leave $V_{1.4}Sb$ as a high-temperature phase.

Structure determination. A single crystal of good quality, synthesized by iodine vapour transport, was used for structure determination. The diffraction data showed systematic absences for *hk*0 with $h + k = 2n + 1$ and for 0*k*0 with $k = 2n + 1$, suggesting either of the two space groups *P*4/*nmm* and *P*4/*n*. The structure was solved on the basis of space group *P*4/*nmm*. Later tests on solving and refining the structure in the lower-symmetry space group *P*4/*n* did not improve the *R*-factor, leaving *P*4/*nmm* as the preferred choice. The major part of the structure was found by application of direct methods (MITHRIL), with difference Fourier syntheses concluding the determination. The atomic parameters and temperature factors are listed in Table 3, and gave $R = 0.030$ and $R_w = 0.031$.

EDX analysis was carried out in order to establish whether traces of iodine were incorporated in the single crystals. The analysis was not conclusive because the signals from Sb and I could not be resolved from each other. Therefore, a repeated structure refinement was performed on data collected for a tiny single crystal which was obtained without using iodine as transporting agent. The refinement of the structure for this crystal, which was of somewhat lower quality, gave $R = 0.044$, $R_w = 0.036$, with no significant changes in the atomic parameters. The latter, small crystals, as well as the V and Sb starting materials, were all checked for possible iodine content, but with negative result. It is concluded that the $V_{15}Sb_{18}$ phase does not contain any iodine.

One of the vanadium sites, V(1) (Table 3), turned out to be only partly occupied, 46(3) and 52(3) %, respectively, for the two single crystals. The composition of both crystals, as judged from the structure determinations, is thus $V_{15}Sb_{18}$.

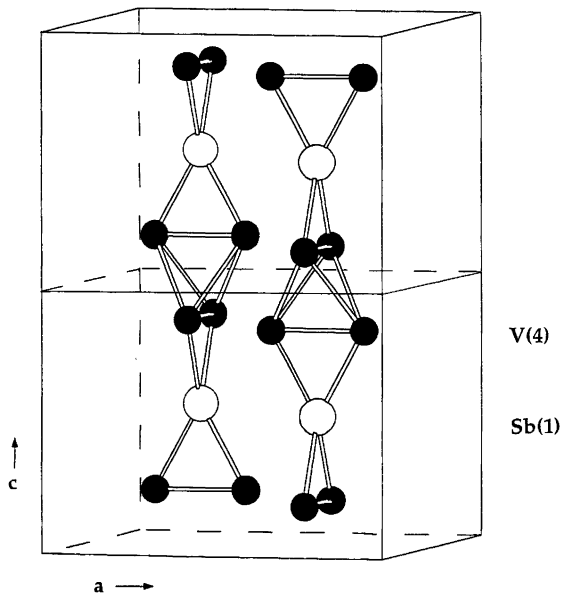

Fig. 1. Schematic representation of $[V(4)_4Sb(1)]_n$ chains in $V_{15}Sb_{18}$. Filled circles, V; open circles, Sb. Two unit cells are shown.

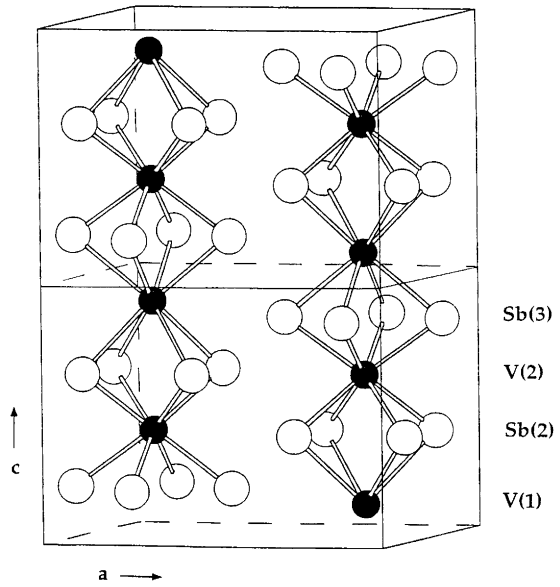

Fig. 2. Schematic representation of $[V(1)V(2)Sb(2)_4Sb(3)_4]_n$ or $[V_2Sb_8]_n$ columns in $V_{15}Sb_{18}$. Filled circles, V; open circles, Sb. Two unit cells are shown.

Atomic arrangement. In the description of the crystal structure, emphasis will be put both on the V–Sb coordination polyhedra and their linking, and on the V–V metal–metal bonding. The crystal structure can, to a first approximation, be described as consisting of two quite different types of columns aligned along the [001] direction. The first type consists of metal tetrahedra formed by the V(4) atoms, which are linked by Sb(1) atoms (Fig. 1). The second type of column consists of approximately square antiprisms of Sb(2) and Sb(3), with alternating V(1) and V(2) atoms in the centers (Fig. 2). The two types of columns are linked by short Sb(3)–V(4) contacts, and in addition via V(3) atoms. Projections of the V sublattice

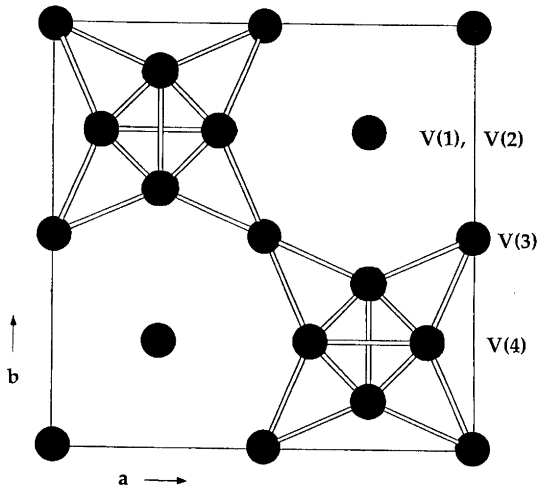

Fig. 3. Projection of the vanadium network (sub-lattice) of $V_{15}Sb_{18}$ on the *ab*-plane.

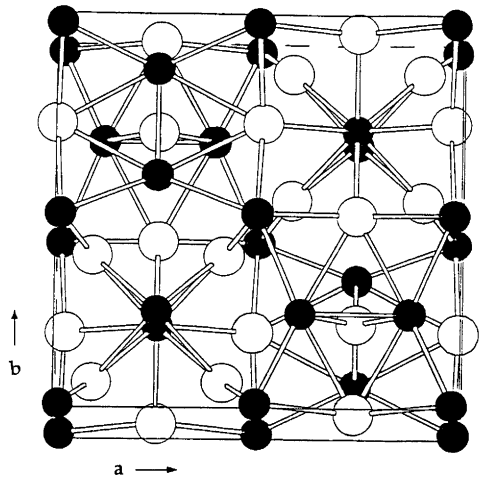

Fig. 4. The crystal structure of $V_{15}Sb_{18}$ as seen along the slightly tilted ***c***-axis. Filled circles, V; open circles, Sb.

and of the crystal structure on the ***ab***-plane are shown in Figs. 3 and 4, respectively.

The intra- and intercolumnar V–Sb distances [272.3(4)–299.7(3) pm; Table 4] are all of normal bonding lengths, and may be compared to e.g. 284.9(4) pm in VSb_2.[7] The Sb–Sb distances larger than 319 pm (Table 4) are considered too long in order to be bonding. The situation for the Sb(2)–Sb(2) bond of 303.6 pm is more uncertain and may be compared with the bonding Sb–Sb distances 289.2(7) pm for the Sb pairs in VSb_2,[7] and with 285.40,[14] 280.7,[15] and 261.7 pm[15] for the Sb four-rings in the Skutterudite-type antimonides $CoSb_3$, $RhSb_3$ and $IrSb_3$, respectively.

Consideration of the V–V interatomic distances (Table 4) indicates that substantial metal–metal bonding occurs in $V_{15}Sb_{18}$. The $V(4)_4$ tetrahedra described above can be considered as integral parts of continuous, two-dimensional nets, formed by V(3) and V(4), with metal–metal interactions existing in the (001) plane. This is illustrated in Fig. 3, where only metal atoms are shown. The V–V interatomic distances are in the range 268.1(1)–

Table 4. Interatomic distances (in pm; $d < 360$ pm) for $V_{15}Sb_{18}$, with calculated standard deviations in parentheses.

V(1)–4 Sb(3)	292.5(3)	Sb(1)–4 V(4)	274.3(1)
V(1)–4 Sb(2)	299.7(3)	Sb(1)–4 Sb(3)	335.4(1)
V(1)–1 V(2)	342.8(5)	Sb(2)–1 V(3)	275.2(6)
V(2)–4 Sb(3)	278.7(2)	Sb(2)–1 V(2)	279.2(2)
V(2)–4 Sb(2)	279.2(2)	Sb(2)–1 V(1)	299.7(3)
V(2)–1 V(1)	342.8(5)	Sb(2)–2 Sb(2)	303.6(1)
V(3)–4 Sb(3)	272.3(4)	Sb(2)–1 Sb(2)	319.0(1)
V(3)–2 Sb(2)	275.2(6)	Sb(2)–2 Sb(3)	353.6(1)
V(3)–4 V(4)	284.9(3)	Sb(3)–2 V(3)	272.3(4)
V(4)–1 Sb(1)	274.3(1)	Sb(3)–1 V(2)	278.7(2)
V(4)–1 Sb(3)	284.6(1)	Sb(3)–1 V(4)	284.6(1)
V(4)–1 V(4)	268.1(2)	Sb(3)–1 V(1)	292.5(3)
V(4)–2 V(3)	284.9(3)	Sb(3)–4 Sb(3)	322.9(1)
V(4)–2 V(4)	294.9(3)	Sb(3)–2 Sb(2)	353.6(1)
		Sb(3)–1 Sb(1)	335.4(1)

294.9(3) pm, which are comparable with metal–metal distances in e.g. pure vanadium (262.2 pm)[16] and VSb_2 (281.9 pm),[7] but significantly longer than the very short chain-forming V–V bonds in the extensive series of vanadium compounds crystallizing in the Cr_3Si (β-W)-type structure, e.g. 247.0 pm in V_3Sb.[2]

Homogeneity region. The structure determinations for two single crystals, prepared by totally different methods, showed both that the V(1) site is partly occupied (roughly half-filled, Table 3). One may speculate whether the $V_{15}Sb_{18}$ phase extends over a wide homogeneity interval ranging between $V_{14}Sb_{18}$ [the V(1) site empty] and $V_{16}Sb_{18}$ [the V(1) site fully occupied]. To answer this question, powder samples with different nominal compositions were carefully prepared. The samples consisted in general of two phases. The observed *d*-values for sets of around 40 Bragg reflections from the $V_{15}Sb_{18}$ phase were chosen for the least-squares refinements. At the V-rich site of the homogeneity region, $a = 958.25$ pm, $c = 705.15$ pm and $V = 647.49 \times 10^6$ pm^3, whereas at the Sb-rich side $a = 958.64$ pm, $c = 704.57$ pm and $V = 647.42 \times 10^6$ pm^3 (average for four samples). As most samples contained minor amounts of neighbouring phases, a definite conclusion as to the composition range cannot be given on the basis of the disappearing phase principle. Since the variation of the unit-cell volume is not significant, the content of the unit cell does not vary to any larger extent, but the significant variations in *a* and *c* prove that the phase has a certain small homogeneity range. This suggests that the $V_{15}Sb_{18}$ phase, for some reason, only exists when the V(1) site is about half-filled. Experiments are presently being undertaken with the aim of introducing other types of metal atoms at the V(1) site.

Structural relationships. The emphasis is first put on the square antiprisms as building units, and on the columns which were considered above (Fig. 2). In $V_{15}Sb_{18}$ and VSb_2 columns of square antiprisms run along the tetragonal axis and are major structural units. In VSb_2, which crystallizes in the $CuAl_2$-type structure, all Sb atoms are situated at the vertices of regular square antiprisms with V atoms in the centers. These antiprisms form columns as in $V_{15}Sb_{18}$, but in VSb_2 all Sb atoms are shared by two columns, which thereby build the entire structure. In $V_{15}Sb_{18}$ the antiprisms are not regular (note that one of the V sites is only partly occupied), but more important, they are not connected to build the whole three-dimensional structure. As pointed out above, the three-dimensional structure in $V_{15}Sb_{18}$ contain two different types of columns plus additional V atoms. Another subtle difference between the square antiprismatic columns in VSb_2 and $V_{15}Sb_{18}$ concerns the V–V contacts, which in VSb_2 probably are bonding,[7] but in $V_{15}Sb_{18}$ are non-bonding.

A schematic comparison of the VSb_2 and $V_{15}Sb_{18}$-type structures is given in Fig. 5, which also includes the crystal structure of VS_4. The one-dimensional VS_4-type structure is built by isolated columns of (distorted) square

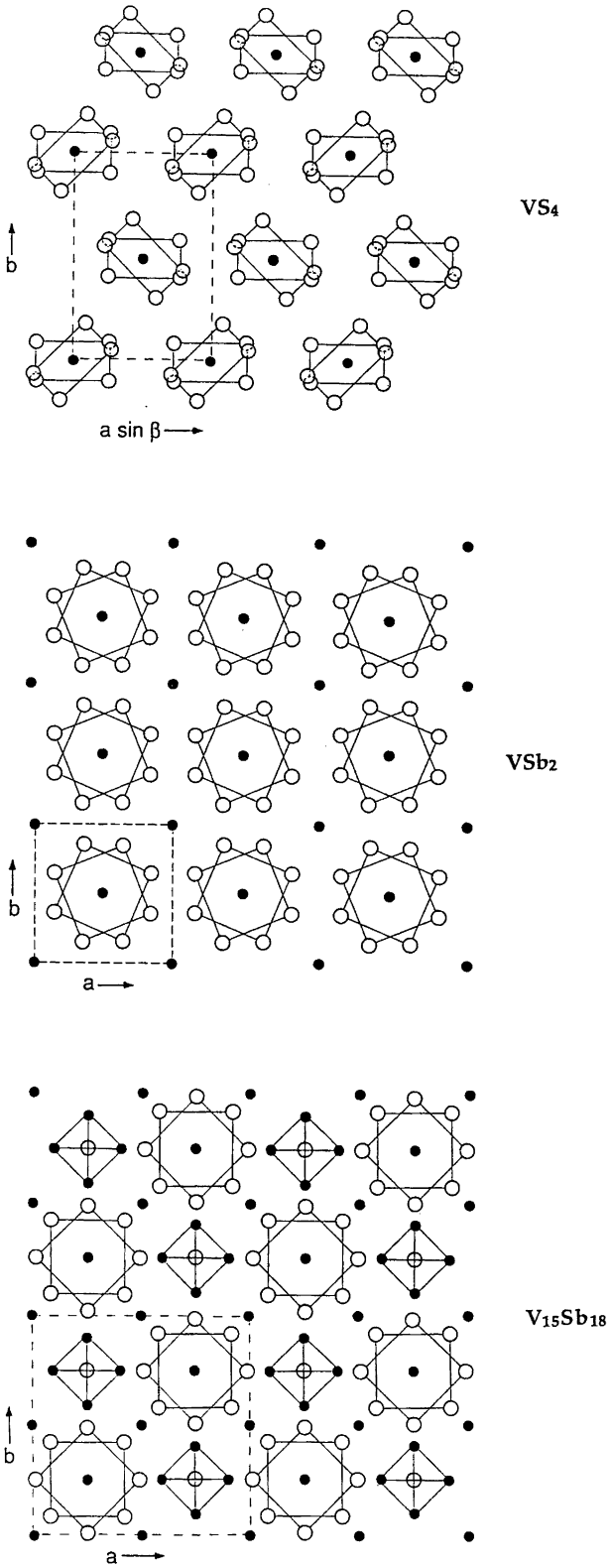

Fig. 5. Schematic representations comparing the crystal structure of VS_4, the $CuAl_2$-type structure of VSb_2, and the $V_{15}Sb_{18}$-type structure. For explanation, see text. Filled and open circles represent metal (V) and non-metal (S, Sb) atoms, respectively.

antiprisms.[17] In VSb_2 the $[V_2Sb_8]_n$ columns are connected, and are in principle not separate units. However, if the connectivity is neglected and only the columns running through the center of the $CuAl_2$-type unit cell are represented, the situation illustrated in Fig. 5 is obtained. Along the [110] direction, $[V_2Sb_8]_n$ columns and $[V]_m$ chains, both running along [001], appear alternately. In the corresponding schematic representation of $V_{15}Sb_{18}$, similar $[V_2Sb_8]_n$ columns (or rather $[V_{1.5}Sb_8]_n$ and $[V]_m$ chains appear in the [110] direction. However, this situation is only found for every second (220) plane. In between, at the (110) planes, chains of $[V_4Sb]_n$ and $[V]_m$ exist. The $V_{15}Sb_{18}$-type structure can hence be described as a $CuAl_2$-type structure where $[V_4Sb]_n$ and $[V]_m$ chains are introduced between two-dimensional units of $[V_2Sb_8]_n$ columns and $[V]_m$ chains.

The second notable structure feature of $V_{15}Sb_{18}$ relates to the metal–metal bonding. The characteristic V_4 tetrahedra found in $V_{15}Sb_{18}$ are also present in the crystal structure of V_3Sb (Cr_3Si or β-W-type, A15),[2] where they are linked to form strings running parallel to the crystallographic axes. Another characteristic feature of the Cr_3Si-type structure is metal atom strings running in three directions (often discussed in connection with superconductivity in this type of phases). This feature is less pronounced for $V_{15}Sb_{18}$, where the metal–metal contacts are two-dimensional in nature, and involves the V_4-tetrahedra and the V(3) atoms (Fig. 3). The metal–metal bonding is extensive in the V pnictides. Chains of metal atoms, notably running only in one direction, are generally found for phases with NiAs-type structure. For $V_{1.4}Sb$[1] the V–V distances in these chains are $c/2 = 272.4$ pm, whereas for VP the NiAs-type atomic arrangement is very atypical owing to an unusually large axial ratio which gives eight V–V separations (four chains) with d(V–V) between 311.2 and 318.0 pm.[18] The MnP-type structure of VAs represents a distorted NiAs-type structure with a three-dimensional network of V–V contacts, with four d(V–V) in the range 291.3–302.4 pm.[18] In the antimonide V_3Sb_2, the V–V bonding is more extensive, and each V has six metal atom neighbours at separations 245.9 (×2), 264.1 (×2) and 309.2 (×2) pm.

There is no apparent similarity between the crystal structure of $V_{15}Sb_{18}$ and Ti_5Te_4. The close relation between the geometry of the corresponding unit cells appears to be accidental. However, a comparison of these structures when projected on the *ab*-plane shows a striking similarity that may provide an explanation why Eberle and Schubert, on the basis of zero-layer Weissenberg film data, came to the wrong conclusion regarding the crystal structure.

Magnetic properties. The magnetic susceptibility shows a slight temperature dependence between 5 and 300 K. The measured susceptibility, i.e. without performing corrections for the core diamagnetism, decreases from 4.4×10^{-6} emu g^{-1} at 5 K to 1.7×10^{-6} emu g^{-1} at 300 K. No evidence for magnetic ordering was found.

Acknowledgements. This work has been supported by The Norwegian Research Council. Thanks are also due to Agnar Aasen, University of Oslo, for assisting with the single-crystal X-ray diffraction measurements.

References

1. Bouwma, J., van Bruggen, C. F. and Haas, C. *J. Solid State Chem. 7* (1973) 255.
2. Rasmussen, S. E. and Grønbæk Hazell, R. *Acta Chem. Scand., Ser. A 32* (1978) 785.
3. Steinmetz, J., Malaman, B. and Roques, B. *C.R. Acad. Sci. Paris, Ser. C 284* (1977) 499.
4. Meissner, H.-G. and Schubert, K. *Z. Metallk. 56* (1965) 523.
5. Grison, B. and Beck, P. A. *Acta Crystallogr. 15* (1962) 807.
6. Eberle, D. and Schubert, K. *Z. Metallk. 59* (1968) 306.
7. Donaldson, J. D., Kjekshus, A., Nicholson, D. G. and Rakke, T. *J. Less-Common Met. 41* (1975) 255.
8. Ersson, N. O. *Program CELLKANT*, Kemiska Intitutionen, Uppsala Universitet, Uppsala, Sweden 1981.
9. Mallinson, P. R. and Muir, K. W. *J. Appl. Crystallogr. 18* (1985) 51.
10. Werner, P.-E., Eriksson, L. and Westdahl, M. *J. Appl. Crystallogr. 18* (1985) 367.
11. de Wolff, P. M. *J. Appl. Crystallogr. 1* (1968) 108.
12. Malmros, G. and Werner, P.-E. *Acta Chem. Scand. 27* (1973) 493.
13. Grønvold, F., Kjekshus, A. and Raaum, F. *Acta Crystallogr. 14* (1961) 930.
14. Schmidt, T., Kliche, G. and Lutz, H. D. *Acta Crystallogr. Sect. C 43* (1987) 1678.
15. Kjekshus, A. and Rakke, T. *Acta Chem. Scand., Ser. A 28* (1974) 99.
16. Schmitz-Pranghe, N. and Dünner, P. *Z. Metallkunde 59* (1968) 377.
17. Allmann, R., Baumann, I., Kotoglu, A., Rösch, H. and Hellner, E. *Naturwissensch. 51* (1964) 263.
18. Selte, K., Kjekshus, A. and Andresen, A. F. *Acta Chem. Scand. 26* (1972) 4057.

Received November 10, 1994.